Title
The conserved AAA-ATPase Msp1 confers organelle specificity to tail-anchored proteins

Journal
Proceedings of the National Academy of Sciences of the United States of America, 111(22)

ISSN
0027-8424

Authors
Okreglak, Voytek
Walter, Peter

Publication Date
2014-06-03

DOI
10.1073/pnas.1405755111

Peer reviewed

The conserved AAA-ATPase Msp1 confers organelle specificity to tail-anchored proteins

Voytek Okreglak and Peter Walter[1]

Howard Hughes Medical Institute and Department of Biochemistry and Biophysics, University of California, San Francisco, CA 94158-2517

Contributed by Peter Walter, March 28, 2014 (sent for review February 11, 2014; reviewed by Thomas Langer and Nikolaus Pfanner)

The accuracy of tail-anchored (TA) protein targeting to the endoplasmic reticulum (ER) depends on the Guided Entry of Tail-Anchored (Get) protein targeting machinery. The fate of TA proteins that become inappropriately inserted into other organelles, such as mitochondria, is unknown. Here, we identify Msp1, a conserved, membrane-anchored AAA-ATPase (ATPase associated with a variety of cellular activities) that localizes to mitochondria and peroxisomes, as a critical factor in a quality control pathway that senses and degrades TA proteins mistargeted to the outer mitochondrial membrane (OMM). Pex15 is normally targeted by the Get pathway to the ER, from where it travels to peroxisomes. Loss of Msp1 or loss of the Get pathway results in the redistribution of Pex15 to mitochondria. Cells lacking both a functional Get pathway and Msp1 accumulate increased amounts of Pex15 on the OMM and display severely dysfunctional mitochondrial morphology. In addition, Msp1 binds and promotes the turnover of a Pex15 mutant that is misdirected to the OMM. Our data suggest that Msp1 functions in local organelle surveillance by extracting mistargeted proteins, ensuring the fidelity of organelle specific-localization of TA proteins.

Correct targeting of proteins to appropriate subcellular compartments is critical for cell organization and physiology. In addition to the well-established signal sequence-directed protein targeting pathways to subcellular organelles (1), some classes of transmembrane proteins use more recently discovered targeting routes. One class comprises tail-anchored (TA) proteins that contain a hydrophobic stretch of amino acids at their extreme C terminus. TA proteins are posttranslationally targeted to the endoplasmic reticulum (ER), mitochondria, and peroxisomes. Many specify organelle identity or are otherwise essential for proper organelle function, including SNAREs, ubiquitin ligases, and organelle division machinery. An ATP-dependent protein targeting pathway [termed the Guided Entry of Tail-Anchored (Get) pathway in *Saccharomyces cerevisiae* (2) and the Asna1/TRC40 pathway in higher eukaryotes (3)] catalyzes insertion of TA proteins into the ER (Fig. 1*A*, WT). In *S. cerevisiae*, the Get pathway is composed of the pretargeting factors Get4, Get5, and Sgt2 which deliver newly synthesized TA proteins from ribosomes to the cytosolic targeting ATPase Get3 (4). TA proteins loaded onto Get3 are then handed off to the ER-resident Get1/Get2 receptor complex, which stimulates the release and insertion of the substrate into the ER membrane (2, 5, 6). The Get pathway also inserts the peroxisomal TA protein factor Pex15 into the ER, from where it is trafficked to peroxisomes as they mature (2, 7).

A dedicated targeting pathway for outer mitochondrial membrane (OMM) TA proteins has not been identified. TA protein targeting to mitochondria is thought to rely on a bipartite topogenic signal composed of a weakly hydrophobic transmembrane segment C-terminally flanked by a small (three to four amino acid) stretch of positively charged residues (8). How these features are recognized and distinguished from those of ER-directed TA proteins remains unclear. In *S. cerevisiae*, the targeting of OMM-localized TA proteins has also been proposed to be guided by the lipid composition of the membrane, in which a low ergosterol content may facilitate the spontaneous insertion of OMM-destined TA proteins (9–11).

The fidelity of partitioning TA proteins between the mitochondria, peroxisomes, and ER is of critical importance to the cell, and as such, ER TA protein targeting is subject to quality control systems that couple failure of membrane integration with substrate ubiquitylation and proteasomal degradation (12). However, the fate of ER TA proteins that escape this preemptive quality control pathway and are mistargeted to the inappropriate organelles is unclear. The observations that disruption of the Get pathway leads to the mistargeting of a subset of ER-destined TA proteins to mitochondria (Fig. 1*A*, *get*Δ and ref. 2) suggests that TA protein targeting to the OMM may be a default targeting pathway that bypasses the quality control systems in place for ER-destined clients. Such a model implies that the OMM would be vulnerable to accumulation of mistargeted proteins, which could become detrimental to mitochondrial function. Thus, we reasoned that a pathway may exist that surveys the OMM, senses mistargeted TA proteins, and promotes their extraction and degradation.

A potential candidate for surveillance of the OMM for mistargeted TA proteins would have two features. First, it would have biochemical characteristics associated with central members of previously defined protein quality control systems, such as Cdc48, an AAA-ATPase that has an essential role in ER-associated protein degradation. Second, it would be localized to the OMM. One such candidate is the highly conserved AAA-ATPase Msp1 (13). Msp1 is an OMM protein containing an N-terminal transmembrane domain followed by a C-terminal cytoplasmic ATPase domain (Fig. 1*B* and ref. 13). High-throughput studies suggest that Msp1 oligomerizes, likely

Significance

Membrane protein targeting to the endoplasmic reticulum, peroxisomes, and mitochondria requires specialized machinery to ensure the appropriate localization of proteins, which is important for defining organelle identity. Additional specificity is provided by sensing and degrading proteins that are mistargeted to an inappropriate compartment. One class of membrane proteins, which contain a hydrophobic segment at their extreme C terminus (called tail-anchored proteins), are prone to be mistargeted; however, how cells cope with this burden is unknown. In this work, we identify a conserved ATPase of the outer mitochondrial membrane, Msp1, which we propose functions as an extraction engine to remove and initiate degradation of an inappropriately targeted tail-anchored protein. In this way, Msp1 serves to enhance the fidelity of protein localization.

Author contributions: V.O. and P.W. designed research; V.O. performed research; V.O. and P.W. analyzed data; and V.O. and P.W. wrote the paper.

Reviewers: T.L., University of Cologne; N.P., University of Freiburg.

The authors declare no conflict of interest.

Freely available online through the PNAS open access option.

See Commentary on page 7888.

[1]To whom correspondence should be addressed. E-mail: peter@walterlab.ucsf.edu.

This article contains supporting information online at www.pnas.org/lookup/suppl/doi:10.1073/pnas.1405755111/-/DCSupplemental.

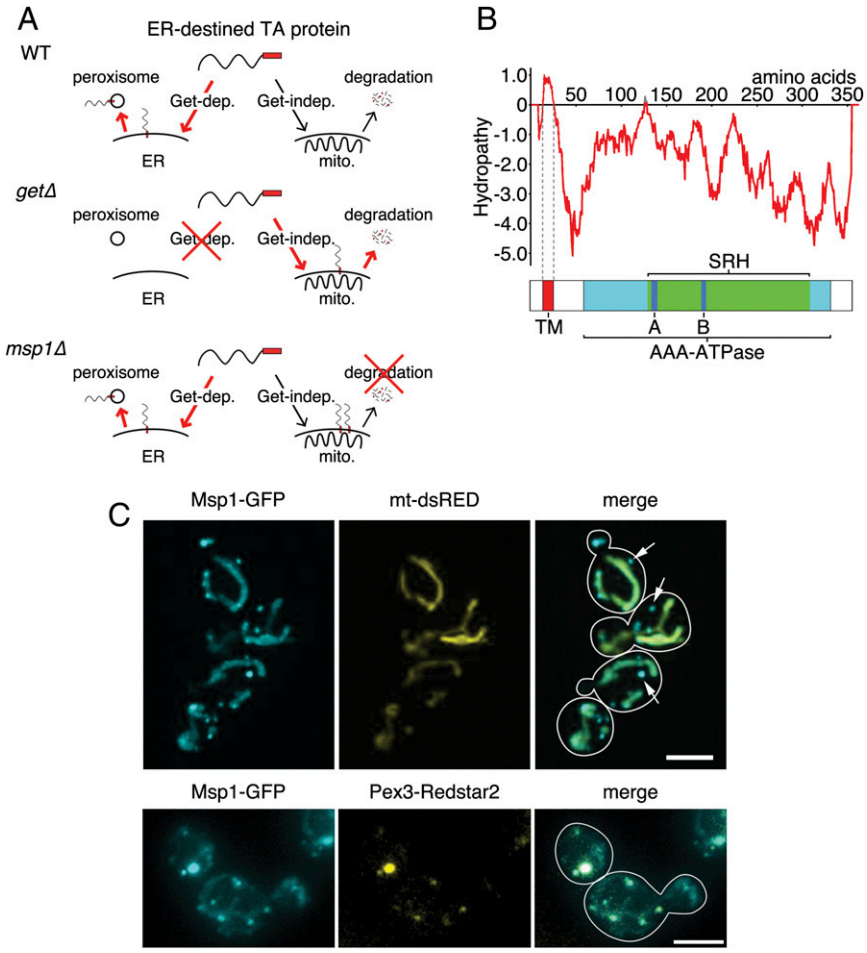

Fig. 1. Msp1 is an N-terminally anchored AAA-ATPase distributed in the mitochondrial outer membrane and peroxisomes. (*A*) WT: A schematic illustrates the Get-dependent targeting of ER-destined TA proteins and the incorporation of specific TA proteins into peroxisomes. Mistargeted TA proteins are sensed and degraded. *get*Δ: In the absence of the dedicated ER-targeting machinery, a subset of ER-destined TA proteins accumulate in the mitochondria, where the degradation machinery becomes important for preventing toxic levels of mistargeted TA proteins from accumulating. *msp1*Δ: In the absence of Msp1, mitochondria accumulate mistargeted ER TA proteins. (*B*) Hydropathy of Msp1 plotted as a function of amino acid calculated from TMpred (www.ch.embnet.org/). A schematic of Msp1 showing predicted structural features is aligned with the hydropathy plot. The Walker A/B and second region of homology motifs are part of the AAA-ATPase conserved module. (*C*, *Upper*) Z-projections of cells expressing chromosomally tagged Msp1-GFP and episomally expressed mt-dsRED. Arrows indicate extramitochondrial Msp1 foci. *Lower*, Z-projections of cells expressing chromosomally tagged Msp1-GFP and Pex3-Redstar2. (Scale bar, 4 μm, applies to all panels.)

into a hexameric structure akin to other AAA-ATPases (14). Unlike Cdc48, which contains two ATPase domains that form a double-ring structure (15, 16), Msp1 contains a single ATPase domain composed of canonical Walker A (P-loop) and B (DExx) motifs (Fig. 1*B*). The presence of a "second region of homology" motif distinguishes Msp1 as a classical AAA-ATPase from the broader AAA^{+}-ATPase superfamily members lacking this domain (17).

In this study, we show that Msp1 is localized to the OMM and to peroxisomes and that it acts to prevent the accumulation of the Get-client Pex15 on mitochondria. Our analyses indicate that Msp1 alleviates mitochondrial-specific stress associated with mistargeted TA proteins by promoting their extraction from the OMM.

Results

Msp1 Is Localized to Mitochondria and Peroxisomes. To localize Msp1, we tagged its gene at its C terminus with green fluorescent protein (GFP) and analyzed the subcellular distribution of the resulting fusion protein by fluorescence microscopy in live cells. In agreement with previous studies (13), Msp1 distributed to mitochondria; however, we also observed numerous extramitochondrial foci that did not colocalize with a red-fluorescent mitochondrial marker (mt-dsRED) (Fig. 1*C*, *Upper*, arrows). To define the extramitochondrial localization of Msp1, we screened for colocalization of Msp1 with other organelle markers. We observed a population of foci in which Msp1 colocalized with the peroxisomal membrane protein Pex3 (Fig. 1*C*, *Lower*), suggesting Msp1 distributes to both peroxisomes and mitochondria. We also observed a minor population of Msp1-positive Pex3-negative foci and, conversely, Msp1-negative Pex3-positive foci, which may represent peroxisomal maturation intermediates.

Msp1 Has a Strong Genetic Interaction with Get Complex Members. Perturbations in the Get pathway cause the mislocalization of several ER- and peroxisome-resident TA proteins to mitochondria (1), thus causing an increased burden of mistargeted proteins. We therefore wondered whether under such conditions a role for Msp1 in monitoring the OMM for mislocalized TA proteins would manifest as genetic interactions affecting the growth rate of the cell. Indeed, high-throughput e-map data suggest strong synthetic-negative genetic interactions of *msp1*

with *get2* and *get3* deletion mutants (18, 19). To expand on these data, we compared the growth of wild-type, *msp1*Δ, *get1*Δ, *get2*Δ, *get3*Δ, and double mutants of *msp1*Δ and each Get pathway member. We observed strong synthetic defects between *msp1*Δ and *get1*Δ, *get2*Δ, and *get3*Δ (Fig. 2*A*, YPD) and less pronounced interactions between *msp1*Δ and *get4*Δ and *get5*Δ (*get4* and *get5* mutants were not pursued further in this work).

The growth phenotypes of the *msp1*Δ *get1*Δ, *msp1*Δ *get2*Δ, and *msp1*Δ, *get3*Δ double-mutant strains were reminiscent of strains defective in mitochondrial respiration. We tested this possibility by analyzing the growth of each double mutant on a nonfermentable carbon source (glycerol), which requires mitochondrial respiration. Consistent with this notion, we observed an enhanced growth defect of the double mutants compared with either single mutant (Fig. 2*A*, YPEG). Unexpectedly, although *msp1*Δ mutant strains did not display a detectable growth defect in these conditions, *get1*Δ, *get2*Δ, and *get3*Δ mutant strains showed substantially impaired growth. These results indicate that a functional Get pathway is important for mitochondrial physiology, perhaps, in part, by preventing mistargeting of normally ER-targeted proteins to the OMM.

Maintenance of normal mitochondrial morphology commonly correlates with accurate inheritance of mtDNA and the ability of cells to grow on nonfermentable carbon sources. We therefore compared the mitochondrial morphology of wild-type, single-mutant, and double-mutant cells (Fig. 2*B*, images). We quantified these morphology defects by binning cells into one of three groups: class 1, tubular, characterized by the elongated, tubular morphology of mitochondria in wild-type cells; class 2, clumped/tubular, characterized as an intermediate morphology in which mitochondria have partially collapsed into clumps but still have mostly wild-type tubules; and class 3, clumped, characterized by collapsed mitochondria with few emanating tubules (Fig. 2*B*, graph). By this criterion, *msp1*Δ mutant cells were indistinguishable from wild-type cells, showing no overt defects in mitochondrial morphology. In contrast, *get1*Δ, *get2*Δ, and *get3*Δ mutant cells showed a distinct morphology defect, displaying mostly class 2 cells. Strikingly, double-mutant cells showed strong synergistic defects displaying mostly class 3 cells. These data suggest that Msp1 acts to alleviate a mitochondria-specific defect imparted by compromised Get-dependent TA protein targeting.

The Loss of Msp1 Function Leads to the Mislocalization of Pex15. As mentioned earlier, a possible explanation for these results is that loss of Msp1 leads to the accumulation of off-pathway targeted Get client proteins to the OMM. To test this notion, we examined the localization of GFP-tagged ER- and peroxisomal-localized TA proteins in *msp1*Δ mutant cells. Screening a collection of 15 protein constructs (listed in *Experimental Procedures*), we found a single protein, GFP-Pex15, that in *msp1*Δ mutant cells displayed a dramatically altered localization compared with wild-type cells: Whereas GFP-Pex15 localized exclusively to peroxisomes in wild-type cells, it also accumulated on mitochondria in *msp1*Δ mutant cells (Fig. 3*A*).

GFP-Pex15 was also mistargeted to the OMM in cells in which the Get pathway was compromised (Fig. 3*B*, *Upper*), in agreement with previous observations (1). To test for synergistic effects with *MSP1* disruption, we examined GFP-Pex15 in *get3*Δ *msp1*Δ double-mutant cells. We found that the accumulation of GFP-Pex15 on the clumped mitochondria was strongly exacerbated (Fig. 3*B*, *Lower*). We obtained indistinguishable results in *get1*Δ *msp1*Δ and *get2*Δ *msp1*Δ double-mutant cells (Fig. S1). Taken together, these data support the notion that Msp1 acts downstream of the Get pathway to clear mistargeted Pex15 from mitochondria.

Overexpression of Msp1 Clears Mistargeted Pex15 from the OMM. If the normal role of Msp1 is to clear mistargeted TA proteins from mitochondria, then the accumulation of mistargeted GFP-Pex15 in *get3*Δ mutant cells (Fig. 3*B*) suggests that Msp1 activity in these cells is insufficient when the normal targeting machinery (i.e., the Get pathway) is compromised. We tested this notion directly by overexpressing Msp1 from the *GAL1* promoter in wild-type and *get3*Δ mutant cells and examining the localization of GFP-Pex15. In wild-type cells, overexpression of Msp1 did not alter the distribution of GFP-Pex15, which was exclusively found on peroxisomes. In contrast, in *get3*Δ mutant cells, Msp1 overexpression caused a striking relocalization of GFP-Pex15 from

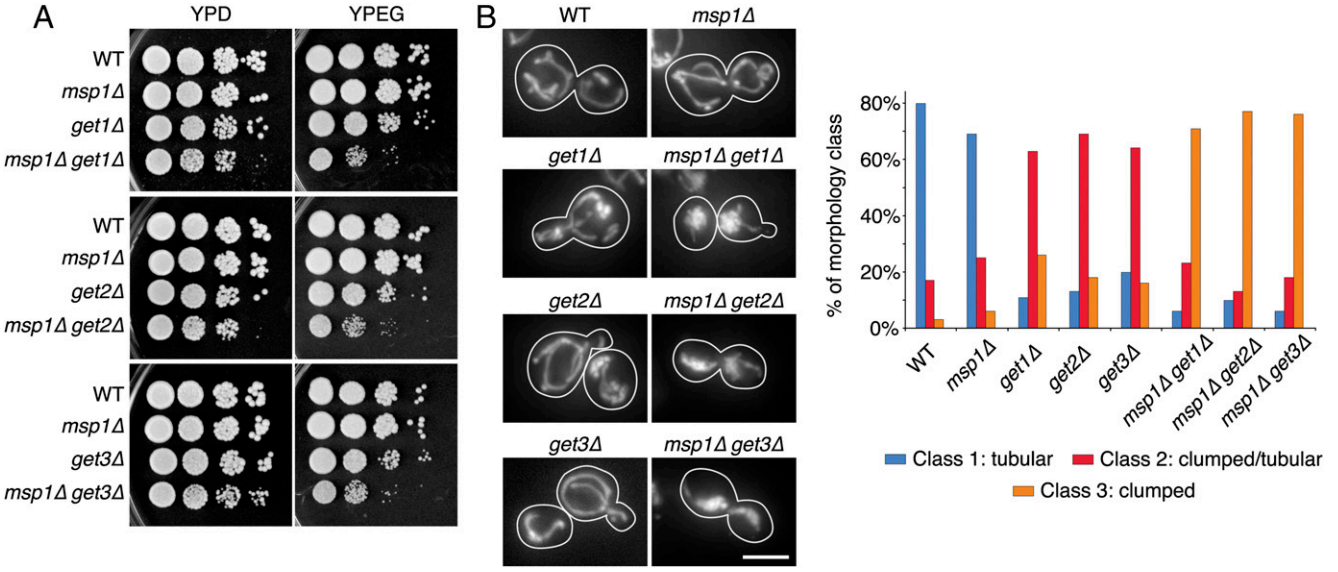

Fig. 2. Msp1 displays synthetic genetic interactions with Get pathway members. (*A*) Serial dilutions of indicated strains spotted on either fermentable dextrose media (YPD) or nonfermentable glycerol media (YPEG). (*B*) Z-projections of indicated strains episomally expressing mt-dsRED grown in selective dextrose media. (Scale bar, 4 μm, applies to all panels.) The bar graph shows distribution of mitochondrial morphologies in wild-type ($n = 29$), *msp1*Δ ($n = 36$), *get1*Δ ($n = 35$), *get2*Δ ($n = 39$), *get3*Δ ($n = 44$), *msp1*Δ *get1*Δ ($n = 34$), *msp1*Δ *get2*Δ ($n = 31$), and *msp1*Δ *get3*Δ ($n = 34$) cells.

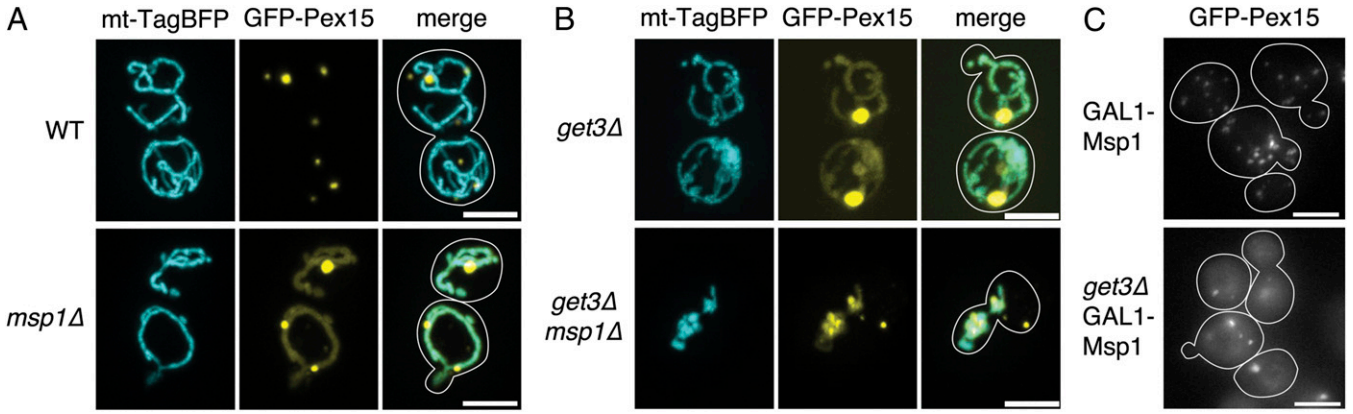

Fig. 3. Msp1 controls the steady-state distribution of Pex15. (*A* and *B*) Z-projections of indicated strains episomally expressing matrix-targeted TagBFP (mt-TagBFP) and GFP-Pex15. (Scale bar, 4 μm.) (*C*) Z-projections of indicated strains episomally expressing GFP-Pex15 grown in inducing conditions (galactose) for 4 h to overexpress Msp1. (Scale bar, 4 μm.)

the OMM into the cytoplasm while leaving GFP-Pex15 localized to peroxisomes unaffected (Fig. 3*C*).

Mistargeted Pex15 Is Cleared More Slowly from Mitochondria in *msp1*Δ Cells. We next asked whether Msp1 acts on mistargeted Pex15 in the presence of a functional Get pathway. To this end, we altered the Pex15 TA-targeting signal to misdirect the protein. Pex15 contains an extended 34-amino acid stretch beyond the transmembrane anchor, which we truncated just beyond a short stretch of basic amino acids (KKYK), creating GFP-Pex15-Δ30. We reasoned that this truncation would create a protein structurally resembling a mitochondrial-targeted TA protein (8). Indeed, when we examined GFP-Pex15-Δ30 localization in wild-type and *msp1*Δ mutant cells, we found that

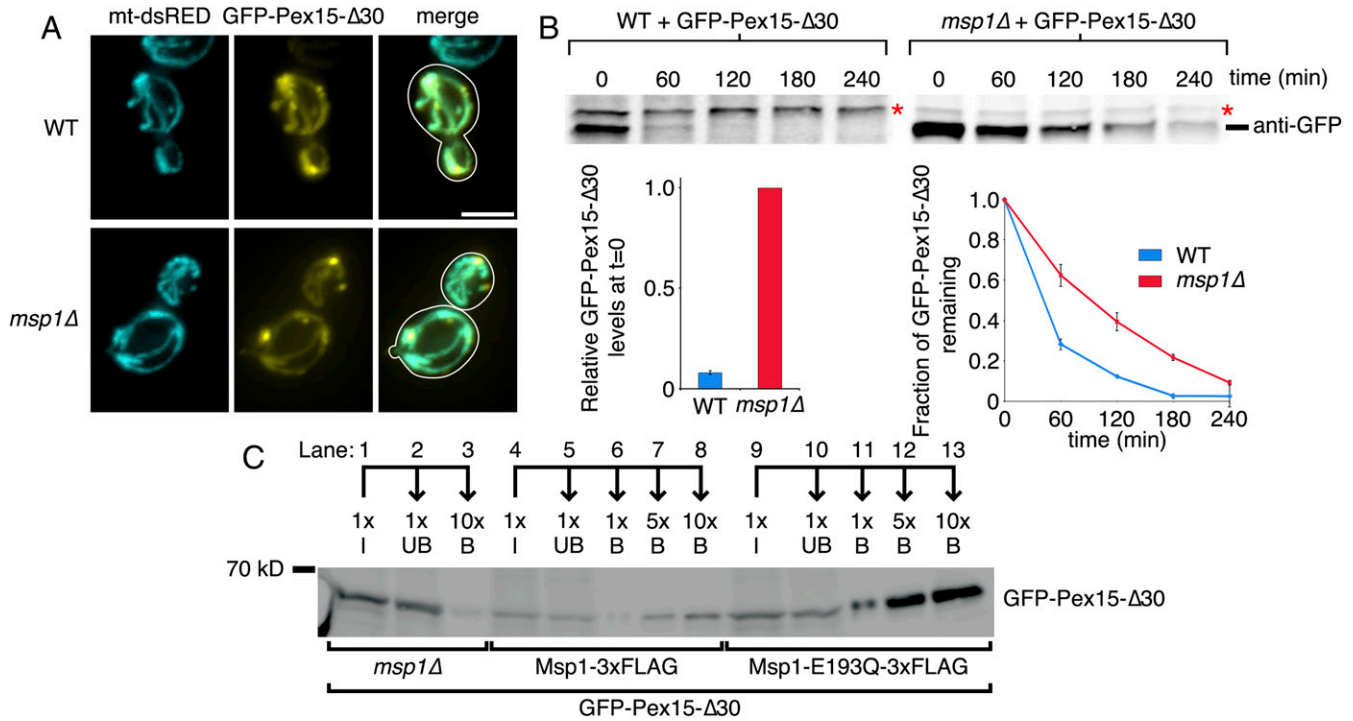

Fig. 4. Msp1 controls the turnover of mistargeted Pex15. (*A*) Z-projections of indicated strains episomally expressing GFP-Pex15-Δ30 under the control of the Gal1 promoter and mt-dsRED. Cells were grown in galactose-containing media for 3 h before imaging. Images are scaled to show the localization of GFP-Pex15-Δ30 and not the relative levels of fluorescent protein. (Scale bar, 4 μm.) (*B*) Wild-type and *msp1*Δ cells expressing GFP-Pex15-Δ30 under the control of the repressible Gal1 promoter were shifted from inducing (galactose) conditions to repressive conditions (dextrose). Cell extracts were prepared at the indicated times after the switch to repressive conditions, subjected to SDS/PAGE, transferred to a PVDF membrane, and blotted with rabbit anti-GFP antibodies to detect GFP-Pex15-Δ30. An infrared imaging system (Licor, Odyssey) was used to detect IRDye-labeled anti-rabbit secondary antibodies. The asterisk indicates a nonspecific band that served as a convenient loading control. The lower left graph shows relative amounts of GFP-Pex15-Δ30 in wild-type and *msp1*Δ cells after 9 h. The normalized relative quantity of GFP-Pex15-Δ30 over time after shifting cells into repressive conditions is shown in the lower right graph. (*C*) Digitonin-solubilized whole-cell extracts from *msp1*Δ cells expressing GFP-Pex15-Δ30 and either Msp1-3xFLAG or Msp1-E193Q-3xFLAG were used as input (I) for immunoprecipitation reactions with anti-FLAG affinity gel. Input samples were separated into unbound (UB) and bound (B) fractions and loaded in the relative amounts shown. Coimmunoprecipitated GFP-Pex15-Δ30 was detected as in Fig. 4*B*.

the truncation caused a marked relocalization to mitochondria (Fig. 4*A*).

We next used GFP-Pex15-Δ30 to probe the clearance of the mutant protein from the mitochondrial membrane. In wild-type cells expressing GFP-Pex15-Δ30 under the control of the regulatable Gal1 promoter, shifting from galactose (inducing) media to dextrose (repressing) media led to the rapid degradation of GFP-Pex15-Δ30 ($t_{1/2}$ = 34 ± 7 min; Fig. 4*B*). In contrast, in *msp1*Δ mutant cells, GFP-Pex15-Δ30 was stabilized, increasing its $t_{1/2}$ ~threefold ($t_{1/2}$ = 87 ± 5 min; Fig. 4*B*). The carbon source switch did not change the doubling times of wild-type or *msp1*Δ mutant cells (wild-type, $t_{1/2}$ = 117 ± 11 min; *msp1*Δ, $t_{1/2}$ = 116 ± 4 min). Taken together with the observation that the levels of GFP-Pex15-Δ30 in wild-type cells at t = 0 were markedly lower (~13-fold) than those in *msp1*Δ mutant cells (Fig. 4*B*, *Left*), these results show that cells containing Msp1 constitutively degrade GFP-Pex15-Δ30.

Msp1 Interacts with Mistargeted Pex15. The stimulation of Pex15-Δ30 degradation in cells containing Msp1 suggested that Msp1 functionally interacts with mistargeted Pex15 to promote its degradation. To test for a physical interaction, we C-terminally tagged Msp1 with 3xFLAG to use in pull-down experiments. We also generated a tagged variant of Msp1 mutated in the Walker B motif (Msp1-E193Q) that, by analogy to other AAA-ATPases, is predicted to impair ATP hydrolysis and trap interactions with putative substrates (20). Expression of Msp1-3xFLAG in *msp1*Δ cells stimulated the turnover of GFP-Pex15-Δ30 (Fig. 4*C*, compare lanes 1 and 4), suggesting the 3xFLAG tag does not impair Msp1 function. In contrast, Msp1-E193Q-3xFLAG did not stimulate the turnover of GFP-Pex15-Δ30 (compare lanes 1 and 9), demonstrating that nucleotide hydrolysis is important for Msp1 function. Immunoprecipitation of Msp1-3xFLAG coprecipitated Pex15-Δ30 (Fig. 4*C*, lanes 6–8), indicating that Msp1 physically interacts with GFP-Pex15-Δ30. The coprecipitation of GFP-Pex15-Δ30 was stimulated ~fivefold (normalized for variable levels of GFP-Pex15-Δ30 in the input) by expressing the substrate trap mutant Msp1-E193Q (compare lanes 6–8 with lanes 11–13). These data suggest that Msp1 binds to mistargeted mitochondrial TA proteins in an ATPase-modulated manner to stimulate their degradation.

Discussion

Proper intracellular protein localization is essential to maintain the compartmentalization of eukaryotic cells. This organization is achieved by the interplay of protein-targeting pathways that recognize features of newly synthesized proteins to bring them to the correct locale and quality control pathways that extract and degrade mislocalized proteins. We here provide evidence that the conserved, integral membrane AAA-ATPase Msp1 is localized to both mitochondria and peroxisomes. We show that on mitochondria, Msp1 plays a role in a previously undescribed pathway that promotes extraction and degradation of the peroxisomal protein Pex15 when it is mistargeted to the OMM (Fig. 1*A*, *msp1*Δ). The role of Msp1 in assuring the correct, peroxisome-specific localization of Pex15 is supported by three lines of evidence. First, loss of Msp1 function leads to the accumulation of Pex15 on the OMM. This result indicates that in normal, wild-type cells, a portion of Pex15 molecules are constitutively mistargeted and that the defect is then corrected by Msp1. Second, in cells where mislocalization of Pex15 to the OMM was exacerbated by compromising the Get pathway (which normally ensures proper Pex15 targeting to the peroxisomes via the ER), Msp1 stimulates the extraction of mistargeted Pex15 in the OMM. Third, Msp1 physically interacts with and accelerates the nucleotide-hydrolysis-dependent turnover of a Pex15 mutant that is inappropriately targeted to the OMM. Although our analyses are focused on a single TA protein, Pex15, Msp1 may similarly act on other mistargeted membrane proteins. Moreover, the dual localization of Msp1 to both the OMM and peroxisomes suggests, by extension, that reciprocally, Msp1 may play a similar role in both organelles.

Precedence for a role of AAA-ATPases in membrane protein extraction is provided by Cdc48, which functions in ER-associated protein degradation and in mitochondrial-associated degradation during conditions of elevated oxidative stress (21). Cdc48 is thought to use the energy of ATP hydrolysis to extract and unfold proteins, readying them for subsequent delivery and degradation by the proteasome. In contrast to Cdc48, Msp1 is predicted to contain only a single hexameric ATPase ring and a bona fide transmembrane segment, which must firmly anchor and orient the oligomeric assembly in the OMM and peroxisomal membrane. Thus, although the use of AAA-ATPases in membrane protein extraction may highlight a common principle of organelle protein surveillance systems, the mechanisms by which Cdc48 and Msp1 perform their respective tasks are likely to be different. In this light, it will be particularly intriguing to assess how Msp1 can distinguish proteins that are in the correct membrane from those that have been mistargeted. A distinguishing feature could be surface determinants that become buried only when the TA protein interacts with partners found exclusively in its appropriate locale. In the absence of such binding partners, these determinants would remain exposed and may be recognized by Msp1 or some cofactor or cofactors yet to be identified, marking the protein for extraction and degradation.

Get pathway mutants, but not *msp1*Δ mutants, display a severely compromised mitochondrial morphology and function (ref. 22 and this study). Thus, Msp1 clears basal levels of mistargeted ER clients during the course of normal growth and becomes limiting when the Get pathway is compromised. Taken together, these data suggest that in wild-type cells, the basal levels of TA protein mistargeting during normal growth is low but may increase when cells are exposed to environmental stresses or nutrient limitation, thus necessitating Msp1 function.

The high degree of homology of Msp1 in eukaryotes suggests that aspects of the TA protein mislocalization sensing pathway described here in *S. cerevisiae* are conserved in higher eukaryotes; however, the role of metazoan Msp1 homologs, ATAD1/Thorase, for this function has yet to be explored experimentally. In support of a similar role in metazoans, ATAD1 has recently been found on peroxisomes (23, 24) and mitochondria (25). In contrast to these similarities, ATAD1 in mouse brains has been suggested to regulate synaptic plasticity and learning by down-regulating postsynaptic AMPA receptors (26), indicating that Msp1 homologs may also have been coopted in evolution for other specialized functions.

Experimental Procedures

Yeast Strains and Plasmids. Yeast strains used in this study are listed in Table S1. Strains with chromosomal integrations were constructed by homologous recombination of PCR products (27). GFP-Pex15 was made by PCR amplifying GFP(S65T) with flanking SpeI and HindIII sites, Pex15 with flanking HindIII and XhoI sites, and cloning both fragments into p416CYC, yielding p416CYC-GFP-Pex15. N-terminal GFP fusions were made to Ubc6, Sec22, Fmp32, Csm4, YBL100C, Use1, Far10, Frt1, Prm3, Pgc1, YDL012C, YBR016W, Gem1, and Fis1, using the same procedure. mt-TagBFP was made by PCR amplifying TagBFP with flanking BamHI and XhoI sites and replacing GFP in pYX113-mtGFP (28), yielding pYX113-mt-TagBFP. An EcoRI/XhoI fragment from pYX113-mt-TagBFP containing the mitochondrial Su9 presequence and TagBFP was subcloned into p413GPD, yielding p413GPD-mt-TagBFP, which was used for this study. GFP-Pex15-Δ30 was made by PCR amplifying GFP-Pex15 lacking the last 30 C-terminal amino acids flanked by SpeI and XhoI sites and cloning into p415GAL1 yielding p415GAL1-GFP-Pex15-Δ30. Msp1-3xFLAG was made by PCR amplifying Msp1 without a stop codon with flanking SpeI and BamHI sites and cloning into p416GAL1, yielding p416GAL1-Msp1. Sense and antisense oligonucleotides encoding 3xFLAG, and a stop codon flanked by sequences complementary to SpeI and BamHI sites were annealed and cloned into p416GAL1-Msp1, yielding p416GAL1-Msp1-3xFLAG.

Msp1-E193Q-3xFLAG was generated using a single oligonucleotide mutagenesis approach, as described (29).

Cell Imaging. Strains were cultivated in SD −Trp lacking the appropriate nutrient for selection of episomal construct at 30 °C at early to midlog phase (OD_{600} ~0.3–0.5), immobilized on coverslips coated with 0.1 mg/mL Con A (Sigma), and imaged using either a Zeiss Axiovert 200M microscope equipped with a 100× 1.3 NA objective and a CCD camera (Orca-ER; Hamamatsu Photonics; Figs. 1*C*, *Lower*, and 2*B*, 3*C*, and 4*A*) or a Nikon Eclipse Ti equipped with a spinning disk confocal (CSU-X1; Yokogawa), EMCCD camera (iXon3 897; Andor), and a 100× 1.49 NA objective (Figs. 1*C*, *Upper*, and 3 *A* and *B*). Images were acquired with μManager software (30) and processed with ImageJ 1.46r (http://rsb.info.nih.gov/ij/). Mitochondrial morphology was classified from maximum-intensity projections, using the following criteria. Cells with tubular (class 1) mitochondria were defined as having no mitochondrial structures more than 600 nm in width, which corresponds to 2 times the average width of a mitochondrial tubule in the majority of wild-type cells under our imaging regime. Cells with clumped/tubular (class 2) mitochondria were defined as having any part of the mitochondrial mass with a diameter more than 600 nm but with more than half of the mitochondrial mass with a width of no more than 600 nm. Cells with clumped (class 3) mitochondria were defined as having any part of the mitochondrial mass with a diameter more than 600 nm but with less than half of the mitochondrial mass with a diameter no more than 600 nm.

Galactose Shutoff Experiment. Cells were grown in SD media for 8 h to the postdiauxic shift (OD_{600} ~1.0), harvested by centrifugation, washed with water, and resuspended in SGal [2% (vol/vol) galactose]. Cells were induced for 9 h, harvested, washed once with water, and resuspended in SD −Leu to $OD_{600} = 0.2$. Cells were harvested every hour and processed to cell extract as per ref. 31, with the following modifications: 1.5×10^8 cells were processed per time point, and cells were boiled in 1% SDS and 100 mM Tris·HCl at pH 7.5 (at 25 °C) for 5 min and then flash-frozen. The cell lysate was rapidly thawed, diluted 10 times with a buffer containing 1% Triton X-100, 150 mM NaCl, 50 mM Tris·HCl at pH 7.5, and left on ice for 10 min. Cell debris was spun down at 10,000 × *g* for 10 min at 4 °C. Lysate from 4×10^6 cells was loaded on an Any kD Mini-PROTEAN TGX gel (Bio-Rad). GFP-Pex15-Δ30 was detected with rabbit anti-GFP antibodies (Invitrogen) and goat anti-rabbit IRDye 680, using an infrared imaging system (Odyssey; LI-COR Biosciences). Quantification of IR signals was performed with Image-Quant 5.2 (GE Healthcare).

Immunoprecipitations. Cells were grown in SD –Leu –Ura to log phase, harvested by centrifugation, washed with water, and resuspended in SGal –Leu –Ura media to $OD_{600} = 0.5$ and grown for 9 h. One hundred OD_{600} units of cells were harvested by centrifugation, washed once with water, and resuspended in ice-cold IP Buffer [50 mM Hepes·KCl at pH 7.5, 50 mM KOAc, 2 mM $Mg(OAc)_2$, 1 mM $CaCl_2$, 200 mM sorbitol, 1 mM NaF, 0.1% digitonin, 1× cOmplete protease inhibitors, EDTA-free (Roche)]. Cells were snap frozen in liquid nitrogen and rapidly thawed in water twice. Glass beads ~0.5 mm in size were added, and the cells were vortexed at 4 °C for 10 min. Cell lysate was removed from the beads, digitonin was added to 1%, and the cell lysate was solubilized at 4 °C for 45 min. Lysate was clarified by centrifugation at 15,000 × *g* for 15 min at 4 °C, and the supernatant was diluted with IP Buffer to 1 mL. Ten microliters of the lysate was harvested for the input lanes (I) of Fig. 4*C*. Twenty-five microliters of Anti-Flag M2 Affinity Gel (Sigma) that had been washed 4× with IP Buffer was added to the diluted lysate and allowed to rotate at 4 °C for 2.5 h. Beads were harvested by centrifugation, and 10 μL of the supernatant was harvested for the unbound lanes of Fig. 4*C*. The beads were washed 4 times with IP Buffer and then boiled in 100 μL Laemmli sample buffer for 5 min to release bound material. Of the bound material, 1 μL (1×), 5 μL (5×), and 10 μL (10×) was loaded on the gel in Fig. 4*C*.

Note Added in Proof. In agreement with our conclusions, Chen et al. (32) independently demonstrated that Msp1 and ATAD1/thorase promote the degradation of mistargeted TA proteins at the OMM.

ACKNOWLEDGMENTS. We thank Dr. Christof Osman, Dr. Margaret Elvekrog, Dr. Carmela Sidrauski, Thomas Noriega, and Dr. Isabelle Le Blanc for critical discussions and comments on the manuscript. V.O. was supported by a Leukemia and Lymphoma Society fellowship. This work was supported by grants from the National Institutes of Health [R01GM32384 (to P.W.)]. P.W. is an investigator of the Howard Hughes Medical Institute.

1. Blobel G (2000) Protein targeting (Nobel lecture). *ChemBioChem* 1(2):86–102.
2. Schuldiner M, et al. (2008) The GET complex mediates insertion of tail-anchored proteins into the ER membrane. *Cell* 134(4):634–645.
3. Stefanovic S, Hegde RS (2007) Identification of a targeting factor for posttranslational membrane protein insertion into the ER. *Cell* 128(6):1147–1159.
4. Wang F, Brown EC, Mak G, Zhuang J, Denic V (2010) A chaperone cascade sorts proteins for posttranslational membrane insertion into the endoplasmic reticulum. *Mol Cell* 40(1):159–171.
5. Wang F, Whynot A, Tung M, Denic V (2011) The mechanism of tail-anchored protein insertion into the ER membrane. *Mol Cell* 43(5):738–750.
6. Mariappan M, et al. (2011) The mechanism of membrane-associated steps in tail-anchored protein insertion. *Nature* 477(7362):61–66.
7. van der Zand A, Gent J, Braakman I, Tabak HF (2012) Biochemically distinct vesicles from the endoplasmic reticulum fuse to form peroxisomes. *Cell* 149(2):397–409.
8. Beilharz T, Egan B, Silver PA, Hofmann K, Lithgow T (2003) Bipartite signals mediate subcellular targeting of tail-anchored membrane proteins in Saccharomyces cerevisiae. *J Biol Chem* 278(10):8219–8223.
9. Krumpe K, et al. (2012) Ergosterol content specifies targeting of tail-anchored proteins to mitochondrial outer membranes. *Mol Biol Cell* 23(20):3927–3935.
10. Kemper C, et al. (2008) Integration of tail-anchored proteins into the mitochondrial outer membrane does not require any known import components. *J Cell Sci* 121(Pt 12): 1990–1998.
11. Brambillasca S, et al. (2005) Transmembrane topogenesis of a tail-anchored protein is modulated by membrane lipid composition. *EMBO J* 24(14):2533–2542.
12. Rodrigo-Brenni MC, Hegde RS (2012) Design principles of protein biosynthesis-coupled quality control. *Dev Cell* 23(5):896–907.
13. Nakai M, Endo T, Hase T, Matsubara H (1993) Intramitochondrial protein sorting. Isolation and characterization of the yeast MSP1 gene which belongs to a novel family of putative ATPases. *J Biol Chem* 268(32):24262–24269.
14. Babu M, et al. (2012) Interaction landscape of membrane-protein complexes in Saccharomyces cerevisiae. *Nature* 489(7417):585–589.
15. Zhang X, et al. (2000) Structure of the AAA ATPase p97. *Mol Cell* 6(6):1473–1484.
16. Huyton T, et al. (2003) The crystal structure of murine p97/VCP at 3.6A. *J Struct Biol* 144(3):337–348.
17. Ogura T, Wilkinson AJ (2001) AAA+ superfamily ATPases: Common structure—diverse function. *Genes Cells* 6(7):575–597.
18. Hoppins S, et al. (2011) A mitochondrial-focused genetic interaction map reveals a scaffold-like complex required for inner membrane organization in mitochondria. *J Cell Biol* 195(2):323–340.
19. Costanzo M, et al. (2010) The genetic landscape of a cell. *Science* 327(5964):425–431.
20. Hanson PI, Whiteheart SW (2005) AAA+ proteins: Have engine, will work. *Nat Rev Mol Cell Biol* 6(7):519–529.
21. Heo J-M, et al. (2010) A stress-responsive system for mitochondrial protein degradation. *Mol Cell* 40(3):465–480.
22. Dimmer KS, et al. (2002) Genetic basis of mitochondrial function and morphology in Saccharomyces cerevisiae. *Mol Biol Cell* 13(3):847–853.
23. Bharti P, et al. (2011) PEX14 is required for microtubule-based peroxisome motility in human cells. *J Cell Sci* 124(Pt 10):1759–1768.
24. Gronemeyer T, et al. (2013) The proteome of human liver peroxisomes: Identification of five new peroxisomal constituents by a label-free quantitative proteomics survey. *PLoS ONE* 8(2):e57395.
25. Pagliarini DJ, et al. (2008) A mitochondrial protein compendium elucidates complex I disease biology. *Cell* 134(1):112–123.
26. Zhang J, et al. (2011) The AAA+ ATPase Thorase regulates AMPA receptor-dependent synaptic plasticity and behavior. *Cell* 145(2):284–299.
27. Janke C, et al. (2004) A versatile toolbox for PCR-based tagging of yeast genes: New fluorescent proteins, more markers and promoter substitution cassettes. *Yeast* 21(11): 947–962.
28. Westermann B, Neupert W (2000) Mitochondria-targeted green fluorescent proteins: Convenient tools for the study of organelle biogenesis in Saccharomyces cerevisiae. *Yeast* 16(15):1421–1427.
29. Pfirrmann T, Lokapally A, Andréasson C, Ljungdahl P, Hollemann T (2013) SOMA: A single oligonucleotide mutagenesis and cloning approach. *PLoS ONE* 8(6):e64870.
30. Edelstein A, Amodaj N, Hoover K, Vale R, Stuurman N (2010) Computer control of microscopes using μManager. *Curr Protoc Mol Biol* Chapter 14:Unit14.20.
31. Zhang T, et al. (2011) An improved method for whole protein extraction from yeast Saccharomyces cerevisiae. *Yeast* 28(11):795–798.
32. Chen YC, et al. (2014) Msp1/ATAD1 maintains mitochondrial function by facilitating the degradation of mislocalized tail-anchored proteins. *EMBO J*, in press.